this example, the number of atomic parameters to be solved is 30, which is smaller than the number of known structure factors, 49. This implies that the problem is in principle solvable. Actually, instead of solving directly the atomic parameters, we derived 141 unknown structure factors beyond 2 Å resolution. The process stopped after 20 cycles of iteration. The discrepancy factor R for the m known structure factors dropped from 0·52 to 0·02, while that for the n unknown ones dropped from 1·0 to 0·36.* The resultant image is shown in Fig. 1(*b*), which shows a prominent enhancement of resolution revealing all the individual atoms. The expected image at 1 Å resolution is shown in Fig. 1(*c*) for comparison.

* The R factor is defined as

$$R = \sum_{\mathbf{H}} |\mathbf{F}_{\mathbf{H}\,\mathrm{true}} - \mathbf{F}_{\mathbf{H}\,\mathrm{estimated}}| \Big/ \sum_{\mathbf{H}} |\mathbf{F}_{\mathbf{H}\,\mathrm{true}}|,$$

where $H \leq H_L$ for the known structure factors and $H > H_L$ for the unknown structure factors. Values of $\mathbf{F}_{\mathbf{H}\,\mathrm{true}}$ are those obtained from Fourier transformation of the structure, while values of $\mathbf{F}_{\mathbf{H}\,\mathrm{estimated}}$ are calculated each cyle from the Sayre equation. The initial $\mathbf{F}_{\mathbf{H}\,\mathrm{estimated}}$ values for the unknown structure factors are all set to zero.

Concluding remarks

The present work confirms the possibility of extracting high-resolution structural information from a low-resolution image. This will be useful not only in electron microscopy but also in diffraction analysis.

An advantage of the method described here is that it does not need any experimental electron diffraction data in addition to an electron micrograph. This is important for radiation-sensitive materials since it makes the experiment simpler to implement. This is also important for enabling the method to be used, at least in theory, for non-crystalline samples.

References

FAN HAI-FU & ZHENG QI-TAI (1975). *Acta Phys. Sin.* **24**, 97-104.
FAN HAI-FU, ZHONG ZI-YANG, ZHENG CHAO-DE & LI FANG-HUA (1985). *Acta Cryst.* A**41**, 163-165.
HAN FU-SON, FAN HAI-FU & LI FANG-HUA (1986). *Acta Cryst.* A**42**, 353-356.
ISHIZUKA, K., MIYAZAKI, M. & UYEDA, N. (1982). *Acta Cryst.* A**38**, 408-413.
LI FANG-HUA (1977). *Acta Phys. Sin.* **26**, 193-198.
SAYRE, D. (1952). *Acta Cryst.* **5**, 60-65.

Acta Cryst. (1988). A**44**, 63-70

Phase Determination Using High-Order Multiple Diffraction of X-rays

BY SHIH-LIN CHANG, HSUEH-HSING HONG, SHAU-WEN LUH, HIASO-HSI PAN AND MAU-CHU TANG

Department of Physics, National Tsing Hua University, Hsinchu, Taiwan 30043

AND JOSÉ MARCOS SASAKI

Instituo de Física, Universidade Estadual de Campinas, Campinas, São Paulo, 13100 *Brazil*

(*Received* 8 *June* 1987; *accepted* 27 *August* 1987)

Abstract

The effect of invariant phases on the intensity profiles of high-order N-beam X-ray diffractions, with $N > 3$, is investigated. Theoretically, the second-order Bethe approximation and the graphic analysis of the structure-factor multiplets involved in the dispersion equation of the dynamical theory of X-ray diffraction are employed to reveal the dominant invariant phases in the multiple diffraction processes. It is shown that the phases of the triplets or the quartets are the effective phases which affect the multiply diffracted intensities. Experimentally, the intensity profiles of four-, five-, six- and eight-beam cases provide clear evidence to support the theoretical considerations.

0108-7673/88/010063-08$03.00

1. Introduction

N-beam multiple diffraction, with $N > 2$, occurs when N reciprocal-lattice points are brought simultaneously onto the surface of the Ewald sphere. The interaction of the N diffracted beams gives rise to a modification of the intensity background of any diffracted beam involved in this N-beam case. Intensity variation near a three-beam X-ray or electron diffraction has been investigated and used to reveal the phase dependence of the diffraction intensities in transmission geometry (Kambe & Miyake, 1954; Hart & Lang, 1961; Post, 1977; Jagodzinski, 1980; Høier & Aanestad, 1981) and in reflection geometry (Colella, 1974; Chapman, Yoder & Colella,

1981; Chang, 1981, 1982*a*, 1986; Juretschke, 1982*a*, *b*; Hümmer & Billy, 1982, 1986; Post, 1983; Gong & Post, 1983; Schmidt & Colella, 1985; Shen, 1986). A recent review (Chang, 1987) on the utilization of this multiple-diffraction technique for phase determination has shown that the sign relation (Chang, 1981, 1982*a*)

$$S_P = \text{sign}\,(\cos\psi_3) = S_L S_R \qquad (1)$$

can be adopted to interpret most three-beam diffraction experiments for phase determination in centrosymmetric crystals. The sign S_L is defined by the intensity distribution near the three-beam diffraction position. S_R is the sign related to the geometry of the involved reciprocal-lattice points with respect to the Ewald sphere. S_P is the sign of the cosine function of the invariant phase ψ_3 of the structure-factor triplet $F_{-H}F_PF_{H-P}$ involved in the three-beam (O, H, P) case. Reflection $H-P$ is the coupling between the primary reflection H and the secondary reflection P. Fig. 1 is a schematic representation of the three-beam (O, H, P) diffraction in reciprocal space. Points O, H and P are the reciprocal-lattice points involved.

Multiple diffraction can be obtained systematically (Renninger, 1937) as follows: The crystal is first aligned for the H reflection so that the end points of the reciprocal vector **H** lie on the surface of the Ewald sphere. The crystal is then rotated around the vector **H** to bring the reciprocal-lattice point P of the secondary reflection onto the surface of the Ewald sphere.

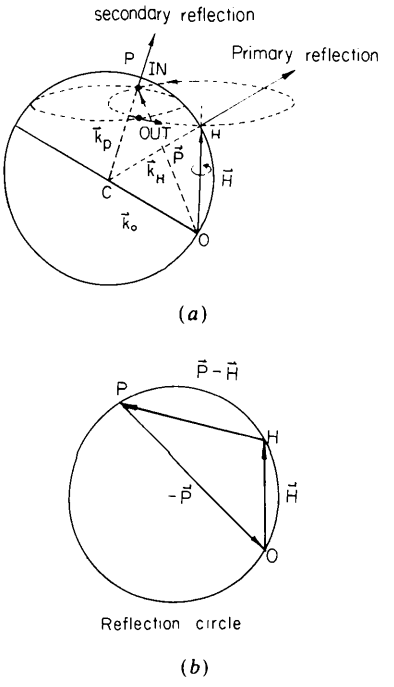

Fig. 1. Schematic representation of a multiple diffraction: (*a*) in reciprocal space and (*b*) in the plane containing the reflection circle.

The wave vectors of the incident, the primary and the secondary reflections are $\mathbf{k}_O$, $\mathbf{k}_H$ and $\mathbf{k}_P$, respectively. The reciprocal-lattice points O, H and P lie on the same reflection circle, as shown in Fig. 1(*b*). The reciprocal-lattice vectors $-\mathbf{H}$, $\mathbf{P}$ and $\mathbf{H}-\mathbf{P}$ connecting the points O, H and P are coplanar. The structure-factor triplet involved in this three-beam case (for a centrosymmetric crystal) is therefore $F_{-H}F_PF_{H-P}$. This can be derived directly from the dispersion relation of the dynamical theory of diffraction. The invariant phase which we are interested in is ψ_3, namely,

$$\psi_3 = \psi_{-H} + \psi_P + \psi_{H-P}, \qquad (2)$$

where ψ_{-H} is the phase of the structure factor F_{-H}.

Useful phase information can, in principle, be extracted also from the diffracted intensities of higher-order N-beam diffractions, with $N>3$. Indications of the phase effect on four-beam diffraction intensities have been observed in transmission geometry (Jagodzinski, 1980) as well as in the Renninger reflection geometry (Post, Gong, Kern & Ladell, 1986). A general four-beam diffraction, however, involves several structure-factor triplets and quartets. How these high-order invariant phases affect the diffraction intensity has not been systematically investigated. A working procedure for phase determination from four-beam and higher-order diffractions is still lacking. It is the purpose of this paper to investigate which multiplet phases play the dominant role in the multiple-diffraction process, and consequently to produce a practical and workable procedure of extracting these dominant phases from experimentally obtained multiple-diffraction line profiles. In this article, we concentrate on the Renninger-type multiple diffraction, where the primary reflection is a symmetric Bragg reflection. The second-order Bethe approximation (Bethe, 1928; Høier & Marthinsen, 1983) is employed to analyse the effect of the high-order structure-factor multiplets on the N-beam diffraction intensity. Experimental evidence is presented to support the theoretical analysis.

2. Theoretical considerations

A. Considerations based on the second-order Bethe approximation

The multiple-diffraction intensity near an N-beam diffraction position can be expressed in terms of an effective structure factor derived from the two-beam approximation in which the secondary reflection is treated as a perturbation to the primary reflection (Juretschke, 1982*a*). Alternatively, the effective structure factor can be directly obtained from the dispersion relation of the dynamical theory of diffraction using the second-order Bethe approximation.

Consider a four-beam diffraction with the four reciprocal-lattice points being O, H, P and Q. The reciprocal-lattice vectors connecting these points are $\mathbf{H}, \mathbf{P}, \mathbf{H}-\mathbf{P}, \mathbf{H}-\mathbf{Q}, \mathbf{P}-\mathbf{Q}$ and their direction-reversed vectors. Following Laue's (1931) treatment, modified by Miyake & Ohtsuki (1974), we can write the fundamental equation of the wave fields in the form

$$2\xi_L \mathbf{E}_L + \sum_{M \neq L} F_{L-M}\mathbf{E}_M = 0 \qquad (3)$$

for $L = O$, H, P and Q. The summation is taken over all the reflections except for L. F_{L-M} and $\mathbf{E}_L$ are the structure factors of the $L-M$ reflection and the Fourier component of the electric field of the L reflection, respectively. The term $2\xi_L$ is defined as

$$2\xi_L = F_O - \gamma^{-1}(K_L^2 - k^2)/k^2, \qquad (4)$$

where $\gamma = r_e\lambda^2/\pi V$. r_e and V are the classical electron radius and the volume of the crystal unit cell. $\mathbf{K}_L$ is the wave vector of the L reflection inside the crystal. k is the magnitude of the incident wave vector, $k = 1/\lambda$, where λ is the wavelength of the X-rays in vacuum.

Each vector equation, (3), should be decomposed into two scalar equations by considering the σ- and the π-polarized components of the wave fields involved and their scalar products. $\hat{\boldsymbol{\sigma}}_L$ and $\hat{\boldsymbol{\pi}}_L$ are the unit vectors of the wave-field components $\mathbf{E}_L$ perpendicular and parallel to the plane of incidence of the L reflection, with $L = O$, H, P and Q. In multi-beam cases (*e.g.* Chang, 1984), $\hat{\boldsymbol{\sigma}}_L$ can be defined as a vector lying on the plane of the reflection circle and tangent to the circle at the reciprocal-lattice point L. $\hat{\boldsymbol{\pi}}_L$ is defined as $\mathbf{K}_L \times \hat{\boldsymbol{\sigma}}_L$. The directions of all the $\hat{\boldsymbol{\sigma}}$'s should be counterclockwise (or clockwise) with respect to the centre of the reflection circle. According to Høier & Marthinsen (1983), the eight scalar equations can be grouped, by neglecting the cross terms $\hat{\boldsymbol{\sigma}}_L \cdot \hat{\boldsymbol{\pi}}_M$, into two sets of four scalar equations, one for σ and the other for π components. The two sets have exactly the same form. This approach is similar to the two-beam approximation proposed by Juretschke (1982*a*). For simplicity, we consider here only the set involving σ components and define $P_{LM} = P_{ML} = \hat{\boldsymbol{\sigma}}_L \cdot \hat{\boldsymbol{\sigma}}_M$.

The fundamental equation of the σ-polarized wave fields has nontrivial solutions for the E's when the following determinant is null:

$$\begin{vmatrix} 2\xi_O & P_{OH}F_{O-H} & P_{OP}F_{O-P} & P_{OQ}F_{O-Q} \\ P_{HO}F_{H-O} & 2\xi_H & P_{HP}F_{H-P} & P_{HQ}F_{H-Q} \\ P_{PO}F_{P-O} & P_{PH}F_{P-H} & 2\xi_P & P_{PQ}F_{P-Q} \\ P_{QO}F_{Q-O} & P_{QH}F_{Q-H} & P_{QP}F_{Q-P} & 2\xi_Q \end{vmatrix} = 0. \qquad (5)$$

This is the dispersion relation of four-beam diffraction. It involves four triplets and three quartets for a centrosymmetric crystal. For a non-centrosymmetric crystal, the numbers of triplets and quartets are doubled, because $F_{-H}F_PF_{H-P} \neq F_HF_{-P}F_{P-H}$.

The 4×4 determinant in (5) can be reduced with suitable approximation to a 2×2 determinant. The dispersion equation becomes

$$\begin{vmatrix} \xi_+ & F_4 \\ F_4' & \xi_- \end{vmatrix} = 0, \qquad (6)$$

where the effective structure factors F_4 and F_4' and the modified resonance failures ξ_+ and ξ_- are defined as

$$\begin{aligned} \xi_+ &= 2\xi_O - \sum_{M=P,Q} P_{OM}^2 F_{O-M}F_{M-O}/2\xi_M \\ \xi_- &= 2\xi_H - \sum_{M=P,Q} P_{HM}^2 F_{H-M}F_{M-H}/2\xi_M \\ F_4 &= F_{O-H}P_{OH} - \sum_{M=P,Q} P_{OM}P_{MH}F_{O-M}F_{M-H}/2\xi_M \\ F_4' &= F_{H-O}P_{HO} - \sum_{M=P,Q} P_{HM}P_{MO}F_{H-M}F_{M-O}/2\xi_M. \end{aligned} \qquad (7)$$

The diffraction intensity I_4 is therefore proportional to the product F_4F_4', *i.e.*

$$I_4 \propto F_4F_4'. \qquad (8)$$

More explicitly, I_4 can be expressed in terms of structure-factor triplets and quartets:

$$\begin{aligned} I_4 \propto\ & F_{O-H}F_{H-O}P_{OH}^2 \\ & - \sum_{M=P,Q} P_3(M)(F_{O-H}F_{H-M}F_{M-O} \\ & + F_{H-O}F_{O-M}F_{M-H})/2\xi_M \\ & + \sum_{M=P,Q}\sum_{L=P,Q} P_4(M,L) \\ & \times F_{O-M}F_{M-H}F_{H-L}F_{L-O}/4\xi_M\xi_L, \end{aligned} \qquad (9)$$

where $P_3(M) = P_{OH}P_{HM}P_{MO}$ and $P_4(M,L) = P_{OM}P_{MH}P_{HL}P_{LO}$. The diffraction intensity I_4 is therefore governed predominantly by the triplet which involves the structure factor F_H of the primary reflection. This statement is supported by the following geometrical consideration related to the actual experimental situation.

The dispersion equation, (5), can be expanded in terms of the structure-factor triplets and quartets. These are graphically depicted as the polygons shown in Fig. 2. The vectors are the reciprocal-lattice vectors which are used to stand for the corresponding structure factors. For example, $\mathbf{H}-\mathbf{P}$ represents the structure factor F_{H-P}. Hence each polygon represents a structure-factor multiplet.

Since the experiments of Renninger type are performed by having the primary reflection planes always in the Bragg diffraction position, the secondary reflection only plays a role as a perturbation to the primary reflection, especially when the crystal is not set at the exact N-beam diffraction position. The interaction between O and H *via* F_H is much stronger than the

interaction between P and Q *via* F_{Q-P}, provided that the H reflection is neither a forbidden nor a very weak reflection. The weak interaction F_{Q-P} is indicated by a dashed vector. Based on this consideration, the triplets A_1 and A_2 have a first-order effect and the multiplets A_3, A_4, A_5 and A_6 have a second-order effect on the diffraction intensity. It should be noted that the phase of A_7 is equal to the phase difference between A_1 and A_2. In the following consideration one will find that both A_1 and A_2 have the same phase. Therefore, A_7 involves no invariant phase.

From this graphical analysis, it is clear that if the primary reflection is neither a forbidden nor a very weak reflection, the intensity variation of a four-beam diffraction provides more information about the triplets A_1 and A_2 than the other multiplets. Moreover, A_1 and A_2 have the same invariant phase, because the triangles A_1 and A_2 are congruent. This can be proven in actual cases in which the phase relations among equivalent reflections are provided by the space group and the geometry of the multiple diffraction. Experimentally, the invariant phase of A_1 can be determined using the sign relation given in (1).

When the structure factor F_H has a very small value, the second-order terms A_3, A_4, A_5 and A_6 become as important as the triplets A_1 and A_2. In this case, all the structure-factor multiplets should be considered in the experimental phase determination. If some forbidden or very weak reflections are involved in the multiplets, the dominant term may be reduced to a triplet or a quartet. Then the determination of the corresponding invariant phase becomes feasible.

The same consideration stated above can be applied to N-beam cases with $N \geq 5$. Equation (9) can be extended to the form

$$I_N \propto F_{O-H}F_{H-O}P_{OH}^2 - \sum_{M\neq O,H} P_3(M) \times (F_{O-H}F_{H-M}F_{H-O} + F_{H-O}F_{O-M}F_{M-H})/2\xi_M + \sum_{M\neq O,H}\sum_{L\neq O,H} P_4(M, L) \times F_{O-M}F_{M-H}F_{H-L}F_{L-O}/4\xi_M\xi_L. \quad (10)$$

The triplets involving F_H (*i.e.* F_{O-H} or F_{H-O}) are still the dominant terms in this intensity expression.

B. Working procedure for phase determination

The proposed sign relation (1) for three-beam diffraction can still be used for phase determination in higher-order multiple diffractions. The sign S_L defined from the intensity line profile is given in Fig. 3. The intensity asymmetry is of course dependent on the way of recording the intensity during the azimuthal rotation. In this investigation our paper chart for intensity recording ran from right to left. The signs S_L are defined according to this experimental arrangement.

The sign S_R of the lattice rotation with respect to the Ewald sphere is defined, in general, as (Chang, 1982*b*)

$$S_R = \text{sign}\,[-\partial\varphi/\partial(1/\lambda)], \quad (11)$$

where φ is the azimuthal angle of rotation. From Cole, Chambers & Duun (1962), a multiple diffraction takes place at the following two azimuthal positions:

$$\varphi = \varphi_0 \mp \beta. \quad (12)$$

The '$-$' and '$+$' signs are for the IN and OUT positions shown in Fig. 1. φ_0 is the initial azimuthal position of the reciprocal-lattice point P of the secondary reflection with respect to the incident plane of the primary reflection H. The angle β is defined as

$$\beta = \cos^{-1}\left[\frac{P^2 - \mathbf{P}.\mathbf{H}}{2P_n\sqrt{(1/\lambda)^2 - H^2/4}}\right], \quad (13)$$

which is half of the angle between the IN and OUT positions in azimuth. p_n is the normal component of the vector **P** to **H**. Since φ_0 is a constant for a given multiple diffraction, S_R can be expressed as

$$S_R = S_\pm \,\text{sign}\,[\partial\beta/\partial(1/\lambda)], \quad (14)$$

where the sign $S_\pm$ is positive for the IN and negative

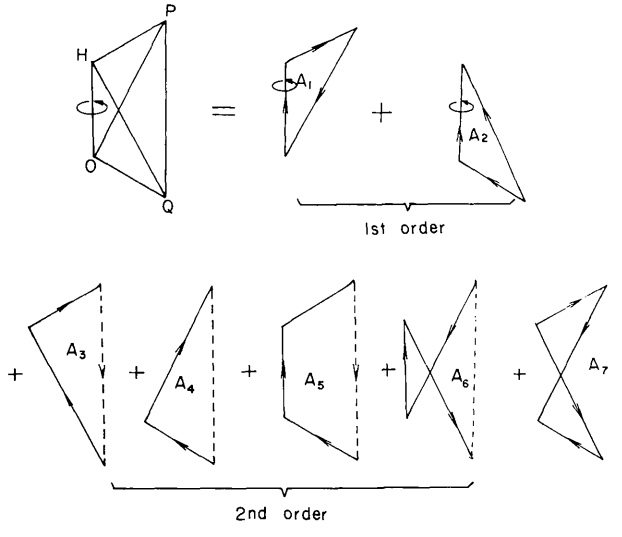

Fig. 2. The structure-factor triplets and quartets involved in a four-beam case of a centrosymmetric crystal.

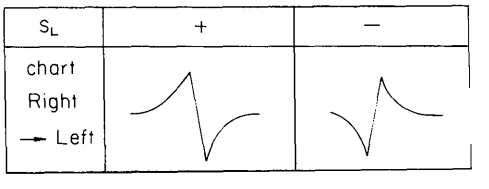

Fig. 3. The definition of S_L.

for the OUT position. From (13), sign $[\partial\beta/\partial(1/\lambda)]$ depends on the sign of $P^2-\mathbf{P}.\mathbf{H}$. The sign S_R in (14) is therefore determined by the product of $S_\pm$ and the sign of $(P^2-\mathbf{P}.\mathbf{H})$, *i.e.*

$$S_R = S_\pm S(P^2-\mathbf{P}.\mathbf{H}). \qquad (15)$$

The sign $S(P^2-\mathbf{P}.\mathbf{H})$ has recently been discussed by Shen (1986). More explicitly, this sign depends on whether the secondary reciprocal-lattice point P lies on the same side or the other side of the bisecting line parallel to $\mathbf{H}$ of the circle of reflection involved. Fig. 4 shows the situations for $S(P^2-\mathbf{P}.\mathbf{H})>0$ and $S(P^2-\mathbf{P}.\mathbf{H})<0$.

From the considerations given above, the following conclusions can be drawn:

When the primary reflection is neither forbidden nor very weak, the following sign relation can be used for phase determination:

$$S_P = \text{sign}\,[\cos\psi_3(A_1)] = S_L S_R, \qquad (16)$$

where $\psi_3(A_1)$ is the phase of the structure-factor triplet A_1 (see Fig. 2).

When the primary reflection is very weak, the experimental phase determination can be carried out by using the relation

$$S_P = \text{sign}\,[\cos\psi_\Sigma] = S_L S_R, \qquad (17)$$

where ψ_Σ is the phase of the dominant structure-factor multiplet. This statement will become obvious when graphical considerations are employed (see § 3 for an example).

3. Experimental results

GaAs crystals were chosen as examples for multiple-diffraction experiments. The known structure information of GaAs (space group $F43m$) facilitates the experimental verification of (16) and (17). A strong reflection (400) and a very weak reflection (200) were used as the primary reflections. Since we are dealing with the sign of $\cos\psi$, only centrosymmetric reflections are considered. Those reflections hkl with $h+k+l=2(2n+1)$ are very weak. Their influence on the structure-factor multiplets is so small that it is neglected in this phase-determination experiment. Consequently, the phase relations of the space group $Fd3m$ can be adopted for phase consideration.

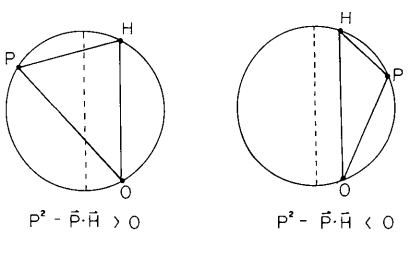

(*a*) (*b*)

Fig. 4. The definition of the sign $S(P^2-\mathbf{P}.\mathbf{H})$.

The experimental setup is the one previously reported by Chang & Valladares (1985). A Rigaku microfocus X-ray generator was used to provide X-rays. The angular divergence of the incident beam was about 3′ arc. Platelike [100]-cut GaAs crystals were prepared. The multiple-diffraction experiments were performed on a Rigaku (manual) single-crystal diffractometer. A chart recorder was employed to record the diffraction intensity. Paper charts ran from right to left.

Figs. 5(*a*) and (*b*) are parts of the GaAs (400) multiple-diffraction scan. The rotation axis is [400]. The mirror positions $\varphi=0$ and $\varphi=45°$ correspond to the positions at which the directions [001] and [011] coincide with the plane of incidence of the primary 400 reflection. The peaks *A*, *B* and *C* are respectively the diffracted intensities of the four-beam (000)(400)(220)(2$\bar{2}$0), the five-beam (000)(400)(5$\bar{1}$1)(244)($\bar{1}$11) and the four-beam (000)(400)(3$\bar{1}$1)(1$\bar{1}$1) cases. Peaks *B*′ and *C*′ are of the five-beam (000)(400)(5$\bar{1}$1)(2$\bar{4}$4)($\bar{1}$11) and the four-beam (000)(400)(31$\bar{1}$)(11$\bar{1}$) diffractions, which are the equivalent diffractions to cases *B* and *C*, respectively. The corresponding IN and OUT parts of these diffractions are also indicated in Fig. 5.

Fig. 5(*c*) shows a part of the GaAs (200) multiple diffraction pattern. Cases *D* and *E* are the six-beam (000)(200)(422)(244)(044)($\bar{2}$22) and the eight-beam

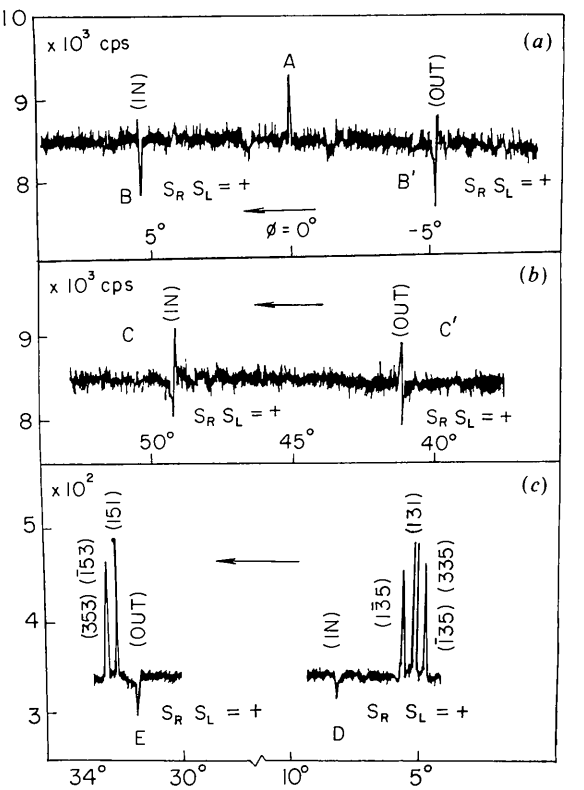

Fig. 5. Multiple-diffraction patterns of GaAs for Cu $K\alpha_1$: (*a*) and (*b*) for the 400 reflection, (*c*) for the 200 reflection.

(000)(200)(402)(404)(206)(006)($\bar{2}04$)($\bar{2}02$) diffractions. The former is at the IN and the latter is at the OUT position.

The structure-factor multiplets involved in these five cases are shown schematically in Fig. 6. Except for case *A*, all the $P_3(M)<0$ and $P_4(M, L)>0$. The diffraction intensity I_N becomes

$$I_N \propto F_{O-H}F_{H-O}P_{OH}^2 + \sum_{M\neq O,H} |P_3(M)| \times (F_{O-H}F_{H-M}F_{M-O} + F_{H-O}F_{O-M}F_{M-H})/2\xi_M + \sum_{M\neq O,H}\sum_{L\neq O,H} |P_4(M, L)| \times F_{O-M}F_{M-H}F_{H-L}F_{L-O}/4\xi_M\xi_L. \quad (18)$$

The sign of each term in (18) is positive. This implies that it is justified to use the 'plus' signs in Fig. 6 to connect all the structure-factor multiplets.

Case *A* is a symmetric case (peak *A* in Fig. 5) in which the secondary reciprocal-lattice point 220 moves towards and $2\bar{2}0$ leaves the Ewald sphere during the azimuthal rotation. This situation corresponds to $S_\pm = 0$. The corresponding $S(P^2 - \mathbf{P}\cdot\mathbf{H})$ is also null. Although the four triplets (a_1, a_2, a_3, a_4) and the three quartets (a_5, a_6, a_7) involve the strong reflections of {220} and {400}, no intensity asymmetry is observed because $S_\pm = 0$. According to (15) and (16), no phase information can be extracted from this intensity profile.

Case *B* (Fig. 6*b*) is a five-beam case in which the reflection 244 and the coupling reflections $244 - 400 = \bar{2}44$ and $511 - \bar{1}11 = 600$ are very weak. If one ignores these very weak reflections, there are two triplets (b_1, b_2), three quartets (b_3, b_4, b_5) and two quintets (b_6, b_7). Based on the discussion given in § 2, only b_1 and b_2 are dominant. Since the triangles b_1 and b_2 are congruent, they involve the same equivalent reflections. According to the phase relation of the space group $Fd3m$, b_1 and b_2 involve the same phase, $\psi_{400} + \psi_{\bar{5}11} + \psi_{1\bar{1}\bar{1}}$. Also, $S_\pm = +$ because the diffraction occurs at the IN position (Fig. 5*a*). The sign $S(P^2 - \mathbf{P}\cdot\mathbf{H})$ is positive owing to $P^2 - \mathbf{P}\cdot\mathbf{H} > 0$. Hence the

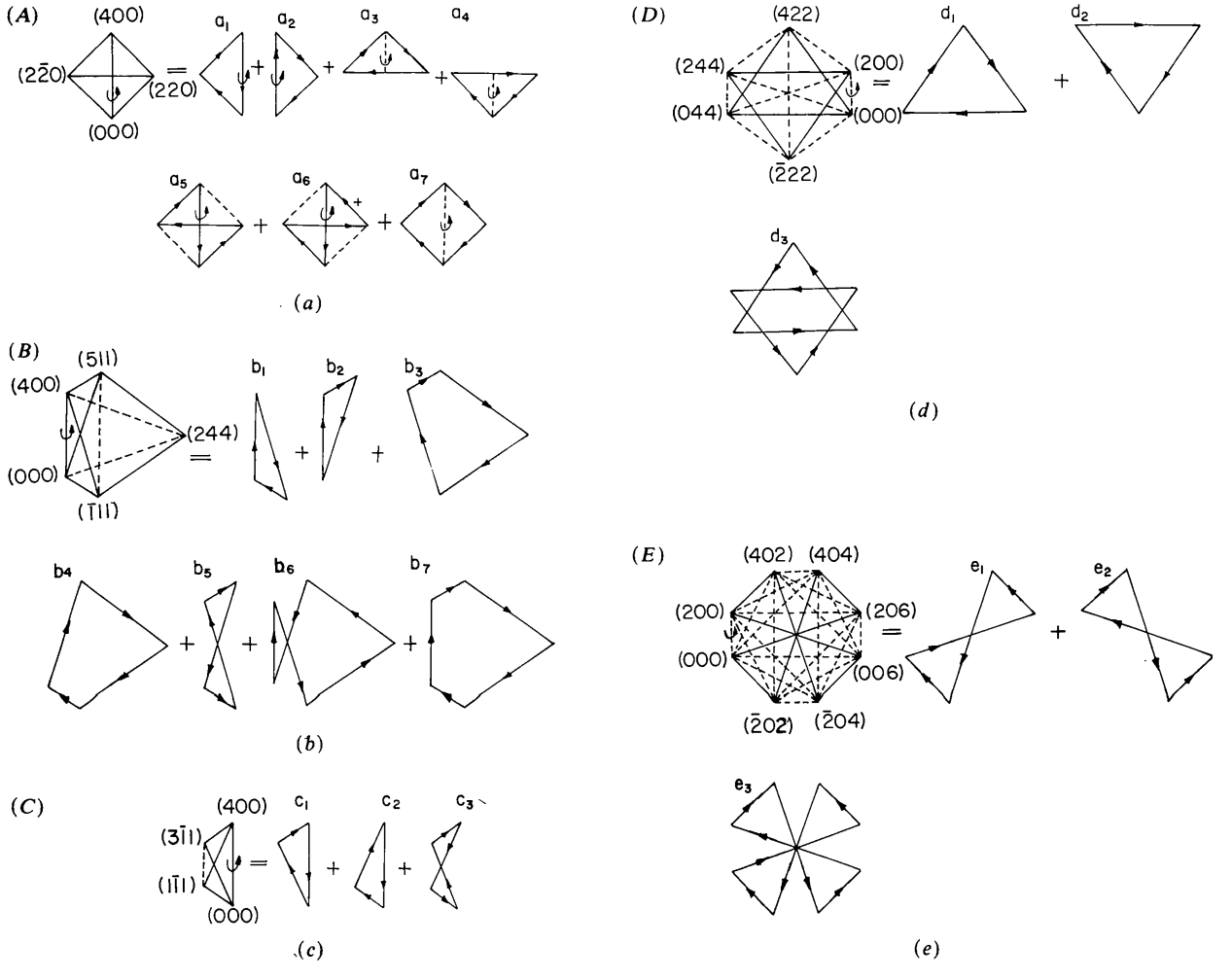

Fig. 6. Structure-factor multiplets involved in the cases *A*, *B*, *C*, *D* and *E*.

Table 1. *Summary of the phase analysis*

Case	$S_\pm$	$S(P^2-\mathbf{P}.\mathbf{H})$	S_R	S_L	S_P	Effective phase
A		0	0		0	
B	+	+	+	+	+	$\psi_{400}+\psi_{\bar{3}11}+\psi_{1\bar{1}\bar{1}}$
C	+	−	−	−	+	$\psi_{400}+\psi_{\bar{1}\bar{1}1}+\psi_{3\bar{1}\bar{1}}$
D	+	+	+	+	+	$\psi_{4\bar{2}2}+\psi_{\bar{4}\bar{2}2}+\psi_{04\bar{4}}$
E	−	+	−	−	+	$\psi_{206}+\psi_{20\bar{2}}+\psi_{\bar{6}0\bar{2}}+\psi_{20\bar{2}}$
B′	−	+	−	−	+	$\psi_{400}+\psi_{\bar{3}\bar{1}1}+\psi_{11\bar{1}}$
C′	−	−	+	+	+	$\psi_{400}+\psi_{\bar{1}1\bar{1}}+\psi_{\bar{3}\bar{1}1}$

sign of rotation S_R is positive, *i.e.* $S_R = S_\pm S(P^2-\mathbf{P}.\mathbf{H}) = +$.

In case *C*, the coupling reflection, $3\bar{1}1-1\bar{1}1 = 200$, is very weak. The effective structure-factor multiplets are the two triplets (c_1, c_2). Both involve the same invariant phase, $\psi_{400}+\psi_{\bar{1}\bar{1}1}+\psi_{\bar{3}1\bar{1}}$. The quartet c_3 is not a dominant factor because it does not involve an invariant phase. Here the phase of c_3 is equal to the phase difference of c_1 and c_2, *i.e.* $\psi_1-\psi_2 = 0°$. This phase difference can also be found analytically from (9). Since $P^2-\mathbf{P}.\mathbf{H}<0$, the sign $S(P^2-\mathbf{P}.\mathbf{H})$ for case *C* is negative.

In case *D* (Fig. 6*d*), the very weak interactions, 200, 244 and 600, are ignored. The case thereby involves the two triplets (d_1, d_2) and a sextet (d_3). The dominant term is d_1. Again d_1 and d_2 have the same invariant phase, $\psi_{4\bar{2}2}+\psi_{04\bar{4}}+\psi_{\bar{4}\bar{2}2}$, the dominant phase. Note that d_3 is a superposition of d_1 and d_2. The sign $S(P^2-\mathbf{P}.\mathbf{H})$ is positive.

In case *E* (Fig. 6*e*), only the two quartets (e_1, e_2) and an octet (e_3) are effective. Here e_1 and e_2 are congruent and e_3 is a superposition of e_1 and e_2. The dominant term in this case is e_1. The corresponding invariant phase is $\psi_{206}+\psi_{20\bar{2}}+\psi_{\bar{6}0\bar{2}}+\psi_{20\bar{2}}$. Since $P^2-\mathbf{P}.\mathbf{H}>0$, $S(P^2-\mathbf{P}.\mathbf{H}) = +$.

Based on the intensity-profile asymmetry of the multiple diffractions *A*, *B*, *C*, *D* and *E* shown in Fig. 4, and the analysis of the effective phases involved in these high-order cases, the signs of the cosines of the effective phases are determined *via* (16). The results are summarized in Table 1. From the last column of this table, we have the relations that the effective phases listed in the table are zero for *A* through *E*. These results are in agreement with the phases calculated directly from the known crystal structure of GaAs.

4. Discussion and concluding remarks

In this paper we have dealt only with the signs of the cosines of the invariant phases. Therefore only the structure-factor multiplets involving centrosymmetric reflections are considered. In GaAs, cases *A*, *B* and *C* are the cases with dominant phases equal to 0°. These multiple diffractions should take place in a centrosymmetric crystal like germanium, for which the lattice constant and crystal symmetry are similar to those of GaAs. As a matter of fact, cases *A*, *B* and *C* have been observed for germanium. The line profiles of these diffractions showed the same intensity asymmetry as those reported here for GaAs [see, for example, Figs. 6.45 and 7.5 of Chang (1984)]. From (16), the corresponding invariant phases are determined as $\psi_{400}+\psi_{\bar{5}11}+\psi_{1\bar{1}\bar{1}} = 0°$ and $\psi_{400}+\psi_{\bar{1}\bar{1}1}+\psi_{\bar{3}1\bar{1}} = 0°$. Since 200 is a forbidden reflection in germanium, there exist no cases *D* and *E*.

Recently Post, Gong, Kern & Ladell (1986) have reported that the phase of an invariant quartet is not necessarily invariant to a change of rotation axis from one twofold axis to another. This conclusion was drawn from the experimental determination of quartet phases directly from the diffraction-intensity asymmetries of the following two four-beam cases of a germanium crystal for Cu $K\alpha_1$: case (I), (000)(222)(315)($\bar{1}\bar{3}1$) with 222 as the primary reflection; and case (II), (000)(444)(351)(13$\bar{1}$) with [444] as the rotation axis. The former involves the structure-factor quartet $F_{222}F_{\bar{4}\bar{4}\bar{4}}F_{1\bar{1}3}F_{13\bar{1}}$ and the latter involves $F_{222}F_{\bar{4}\bar{4}\bar{4}}F_{1\bar{1}3}F_{13\bar{1}}$. The phases of these two quartets are the same, namely $\psi_4 = 0°$. However, the intensity line profiles showed opposite asymmetries [see Fig. 7 of Post, Gong, Kern & Ladell (1986)]. Note that one case was at the IN and the other at the OUT position. The paper chart ran from left to right. The variation of invariant phases due to the difference in the rotation axis was therefore concluded.

These two cases are re-analysed here in the light of the considerations of § 2. From (9) and the graphic analysis (see Fig. 2), the dominant phases in cases (I) and (II) are $\psi_3 = \psi_{222}+\psi_{1\bar{1}3}+\psi_{\bar{3}\bar{1}\bar{5}}$ and $\psi_3 = \psi_{444}+\psi_{\bar{1}\bar{1}\bar{3}}+\psi_{\bar{3}\bar{5}\bar{1}}$, respectively. The former is equal to 180° and the latter to 0°. These phases are consistent with the opposite asymmetry in intensity obtained experimentally. Hence, all the signs S_L, S_R and $S(\cos\psi_3)$ of both cases follow the sign equation (16).

This analysis also shows that the dominant invariant phase involved in a high-order multiple diffraction does not vary, no matter what rotation axis is chosen.

In conclusion, we have discussed the effect of the high-order structure-factor multiplets on the diffraction intensities of *N*-beam cases with $N>3$. The second-order Bethe approximation and the graphic analysis have been employed in the discussion. It is found that the dominant phase in a high-order multiple diffraction is the triplet-invariant phase ψ_3 which involves a non-forbidden primary reflection. The sign of $\cos\psi_3$ can be determined experimentally *via* (16). When the primary reflection is very weak, the dominant phase may not be the triplet phase. In this case, the dominant structure-factor multiplet can be found by the graphic analysis. The corresponding invariant phase is then determined *via* (17). Therefore, both (16) and (17) can serve as the working relations for extraction of phase information from high-order diffractions.

The authors are indebted to the National Science Council of the Republic of China for financial support through grant NSC76-0208-M007-30. JMS acknowledges also the Conselho Nacional de Pesquisas e Desenvolvimento of Brazil for providing a graduate fellowship.

References

BETHE, H. (1928). *Ann. Phys. (Leipzig)*, **87**, 55-129.
CHANG, S. L. (1981). *Appl. Phys.* A**26**, 221-226.
CHANG, S. L. (1982*a*). *Phys. Rev. Lett.* **48**, 163-166.
CHANG, S. L. (1982*b*). *Acta Cryst.* A**38**, 516-521.
CHANG, S. L. (1984). *Multiple Diffraction of X-rays in Crystals.* Berlin, Heidelberg, New York, Tokyo: Springer-Verlag.
CHANG, S. L. (1986). *Phys. Rev. B*, **33**, 5848-5850.
CHANG, S. L. (1987). *Crystallogr. Rev.* **1**, 87-189.
CHANG, S. L. & VALLADARES, J. A. P. (1985). *Appl. Phys.* A**37**, 57-64.
CHAPMAN, L. D., YODER, D. R. & COLELLA, R. (1981). *Phys. Rev. Lett.* **46**, 1578-1581.
COLE, H., CHAMBERS, F. W. & DUUN, H. M. (1962). *Acta Cryst.* **15**, 138-144.
COLELLA, R. (1974). *Acta Cryst.* A**30**, 413-423.
GONG, P. P. & POST, B. (1983). *Acta Cryst.* A**39**, 719-724.
HART, M. & LANG, A. R. (1961). *Phys. Rev. Lett.* **7**, 120-121.
HØIER, R. & AANESTAD, A. (1981). *Acta Cryst.* A**37**, 787-794.
HØIER, R. & MARTHINSEN, K. (1983). *Acta Cryst.* A**39**, 854-860.
HÜMMER, K. & BILLY, H. W. (1982). *Acta Cryst.* A**38**, 841-848.
HÜMMER, K. & BILLY, H. W. (1986). *Acta Cryst.* A**42**, 127-133.
JAGODZINSKI, H. (1980). *Acta Cryst.* A**36**, 104-116.
JURETSCHKE, H. J. (1982*a*). *Phys. Rev. Lett.* **48**, 1487-1489.
JURETSCHKE, H. J. (1982*b*). *Phys. Lett. A*, **92**, 183-185.
KAMBE, K. & MIYAKE, S. (1954). *Acta Cryst.* **7**, 218-219.
LAUE, M. VON (1931). *Ergeb. Exakten Naturwiss.* **10**, 133-158.
MIYAKE, S. & OHTSUKI, Y. H. (1974). *Acta Cryst.* A**30**, 103-104.
POST, B. (1977). *Phys. Rev. Lett.* **39**, 760-763.
POST, B. (1983). *Acta Cryst.* A**39**, 711-718.
POST, B., GONG, P. P., KERN, L. & LADELL, J. (1986). *Acta Cryst.* A**42**, 178-184.
RENNINGER, M. (1937). *Z. Phys.* **106**, 141-176.
SCHMIDT, M. C. & COLELLA, R. (1985). *Phys. Rev. Lett.* **55**, 715-717.
SHEN, Q. (1986). *Acta Cryst.* A**42**, 525-533.

Acta Cryst. (1988). A**44**, 70-75

Electron Diffraction Patterns of Chrysotile: Effect of Specimen Orientation

BY J. E. CHISHOLM

Department of Mineralogy, British Museum (Natural History), Cromwell Road, London SW7 5BD, England

(*Received* 16 *May* 1987; *accepted* 17 *September* 1987)

Abstract

Electron diffraction patterns of chrysotile asbestos fibrils should have the $2mm$ symmetry of a rotation photograph because the layers in the structure are curled as cylinders. The way in which the fibril orientation affects the diffraction patterns is considered theoretically. The departures from ideal symmetry attributable to specimen orientation are noted: they affect mainly the $h00$ reflections close to the fibre axis. Actual diffraction patterns show a consistent difference in the separation of the $h0l$-$h0\bar{l}$ pairs on the upper levels, and $\bar{h}0l$-$\bar{h}0\bar{l}$ pairs on the lower. The experimental conclusion [Yada (1979). *Can. Mineral.* **17**, 679-691] that this difference is not an effect of specimen orientation is confirmed theoretically but its cause remains obscure.

Introduction

The serpentine minerals are hydrated magnesium silicates, $Mg_3Si_2O_5(OH)_4$, with structures which consist of composite layers parallel to (001). In these, a layer of SiO_4 tetrahedra shares the apical oxygen atoms with a layer of $Mg(OH,O)_6$ octahedra. However, the octahedral magnesium hydroxide layer has a and b dimensions which are a little larger than those of the silicate layer. The resulting strain is relieved by curling of the composite layers with the (larger) magnesium hydroxide layer on the outside. In the variety of serpentine known as chrysotile, the composite layers curl about the a axis and wrap around this axis to form the tiny cylinders which are the asbestos fibrils.

The theory of diffraction from cylindrical lattices (and arrangements related to them, such as spirals and helices) was developed by Jagodzinski & Kunze (1954) and in a series of papers by Whittaker (1954, 1955*a*, *b*, 1956, 1957, 1963), who also determined the detailed atomic arrangement in chrysotile. X-ray fibre diffraction photographs, and later electron diffraction patterns, showed the features expected for cylindrical wrapping of the composite layers. Whittaker's deductions were strikingly confirmed by the high-resolution electron micrographs of Yada (1967, 1971) which showed directly the wrapping of the layers about the axis of the cylindrical fibrils.

The wrapping of layers around the axis of a cylinder implies that diffraction patterns from a stationary fibre should have the $2mm$ symmetry of a rotation photograph. X-ray fibre patterns do indeed have this

0108-7673/88/010070-06$03.00